Understanding Malaria Induced Red Blood Cell Deformation Using Data-Driven Lattice Boltzmann Simulations

Joey Sing Yee Tan[1], Gábor Závodszky[2], and Peter M. A. Sloot[1,3,4(✉)]

[1] Complexity Institute, Nanyang Technological University, 50 Nanyang Avenue, 639798 Singapore, Singapore
[2] Computational Science Laboratory, Faculty of Science, Institute for Informatics, University of Amsterdam, Amsterdam, Netherlands
[3] Computational Science, University of Amsterdam, Science Park 904, 1098 XH Amsterdam, Netherlands
p.m.a.sloot@uva.nl
[4] National Research University ITMO, St. Petersburg, Russia

Abstract. Malaria remains a deadly disease that affected millions of people in 2016. Among the five Plasmodium (P.) parasites which contribute to malaria diseases in humans. P. falciparum is a lethal one which is responsible for the majority of the world-wide-malaria-related deaths. Since the banana-shaped stage V gametocytes play a crucial role in disease transmission, understanding the deformation of single stage V gametocytes may offer deeper insights into the development of the disease and provide possible targets for new treatment methods. In this study we used lattice Boltzmann-based simulations to investigate the effects of the stretching forces acting on infected red blood cells inside a slit-flow cytometer. The parameters that represent the cellular deformability of healthy and malaria infected red blood cells are chosen such that they mimic the deformability of these cells in a slit-flow cytometer. The simulation results show good agreement with experimental data and allow for studying the transportation of malaria infected red blood cell in blood circulation.

Keywords: Malaria-infected red blood cells · Lattice Boltzmann
Stage V gametocyte

1 Introduction

In spite of treatment with new antimalarial combinations and enhanced vector control, malaria remains as a deadly disease in Africa, South-East Asia and Eastern Mediterranean. Malaria affected more than 200 million people in 2016 and caused about 445000 deaths based on recent WHO World Malaria 2017 report [33]. Among the five Plasmodium (P.) parasite species which contribute to malaria disease in humans, P. falciparum is a lethal one which is responsible for the majority of the world-wide-malaria-related deaths [1, 8]. In an effort to disrupt parasite transmission, the WHO has developed a global technical strategy for malaria (2016–2030), which shifts their focus from disease control to elimination. These parasites are transmitted

Y. Shi et al. (Eds.): ICCS 2018, LNCS 10860, pp. 392–403, 2018.
https://doi.org/10.1007/978-3-319-93698-7_30

among humans by the female Anopheles mosquito vector. The complex life cycle of P. falciparum is associated with a 44–48 h of asexual replication which takes place in the human host. The parasite in the form of merozoite invades healthy red blood cells (hRBC) and matures through the ring, trophozoite and schizont stages. After the first asexual cycle, a subset of these asexual parasites ($\sim$0.1%–5%) develop into male and female gametocytes, known as gametocytogenesis cycle which takes about 10–14 days to mature [13, 27]. Although these gametocytes do not directly contribute to malaria pathology, they play vital role in completing its life cycle by transmitting parasites to mosquito vector.

Gametocytogenesis consists of five distinct stages where the mid-stage (II–IV) gametocytes show low deformability and are sequestered into deep tissues such as bone marrow and spleen cords to avoid clearance by the spleen [8, 22]. Several studies have shown that only the mature banana-shaped stage V gametocytes (vRBC) are able to move freely in the peripheral blood circulation [13, 22, 27, 28]. In 1880, Laveran first found this banana-shaped stage V gametocyte in the blood smear of an Algerian malaria patient through microscopic technique [21]. The cellular deformability switching of the mature gametocytes is correlated to the morphological alterations, where a protein resident tends to modify the arrangement of inner membrane complex after invasion [1, 7, 8, 28]. Experimental studies have suggested that the SubTelomEric Variable Open Reading frame (STEVOR) proteins contribute to the overall stiffness tuning [28]. The underlying mechanisms of shape shifting and increment of cellular deformability is due to the linkage disassociation of STEVORs from the RBC membrane with mature stage V gametocytes. Since the banana-shaped stage V gametocyte is the only reproduction factor, studies of the deformation characteristics of single stage V gametocyte can offer insights into the connections among mechanical state, especially how well it deforms to sequester in the subdermal micro capillaries of skin where they are easily accessible to mosquito during blood meals.

Due to the significant improvement in developing high fidelity patient specific models for blood flow simulation, several macroscopic open-source software has been developed and available freely for researchers. For instance, CVSim (CardioVascular Simulator), SimVascular, and HemoCell (High pErformance MicrOscopic CELlular Library). CVSim models the human cardiovascular system as a lumped-parameter model and it has been used for research and teaching quantitative physiology courses at MIT and Harvard Medical School [14]. CVSim focuses on the normal physiology and pathology of the cardiovascular system. Similarly, SimVascular is another open source software which serves as a platform for cardiovascular simulation [10]. Both CVSim and SimVascular are good for cardiovascular simulation, but they are not useful for application on cellular level and multi-scale modelling. HemoCell, on the other hand, implements multi-scale in-silico modelling for arterial health and diseases [15]. The design of HemoCell allows the user to extend in-silico studies for cellular level of blood suspension with various types of cells and transport mechanisms of single cells in micro-fluidic setting [34]. In addition, the high computational performance enables applications up to macroscopic scales.

In this paper, HemoCell serves as the framework to replicate the stretching forces acting on a cell inside a slit-flow cytometer where the parameters used in representing the cellular deformability of hRBC and vRBC are being tuned in order to obtain the

respective optimal parameters values which best fit to mimic the deformability of the cell. The tuned parameters include membrane viscosity (η_m) and elasticity (κ_L) which characterize the cellular deformability and viscoelasticity in shear flow, with a shear stress of 3 Pa. Apart from that, we adopted the exact dimensional measurement from previous research [1] to represent a reliable three-dimensional object for vRBC.

2 Methodology

2.1 Computational Methods

Computational fluid dynamics (CFD) will be used to obtain a more detailed understanding on the biomolecular interactions in blood fluid. Especially in the complex system which involves microscopic interaction of healthy, and malaria-infected red blood cells in blood plasma; such as stretching of the red blood cells due to high shear stress or compression arising from differential pressure. The full simulation of the microscopic interaction between blood plasma and red blood cells is challenging as it does not only involve complex geometries but also highly complex multi-scale physics. For this purpose, we chose a powerful approach known as the lattice Boltzmann method (LBM). In the last two decades, LBM has been widely implemented in several applications, including flow through porous medium [24], wind-driven ocean circulation [26, 35], discontinuous flows with shocks [36, 37], tidal flows on complex geometries with irregular bathymetry [29], microscopic interactions in capillary flow [11, 18–20], blood flow simulations involving time harmonic and pulsatile flows [3–5], and also corals studies [16].

LBM is well-known among scientific computing as the method itself is based on statistical physics and discretized particle velocities in accordance to restricted physical spaces. For instance, in the three-dimensional Lattice BGK model, a particle can only move along 19 directions, including the one staying at rest. Excellent parallelisations of the LBM methods do exist, especially the simulation of flows in complicated geometries [6, 17, 31, 32]. We employed HemoCell [38], where the blood plasma is modelled as an incompressible Newtonian fluid and where the lattice Boltzmann method is used to solve the fluid flows. For this purpose, a fully parallelized LBM-based fluid solver library known as Palabos is utilized to produce accurate flow results in microvascular settings. Both the surfaces of hRBC and vRBC are modelled using the discrete element method, where the boundary layers are immersed into the plasma via Immersed Boundary method (IBM) [34]. These membranes are modelled using discrete element methods where edges, N_e connecting the vertices N_v yielding surface triangles N_{tri}. In our simulations, the membranes of hRBC and vRBC consists of $N_v = 642$; 260 vertices, $N_e = 1920$; 778 edges, and $N_{tri} = 1280$; 516 faces, respectively.

The computational efficiency of HemoCell has been demonstrated recently [2] where comprehensive studies has been done to investigate the fractional load imbalance overhead in a high-performance biofluid simulation. The authors found that in the three-dimensional domain decomposition, the fractional load imbalance overhead was

smaller than the fractional communication overhead. Results showed good agreement between the measurements and their load imbalance model.

2.2 Modelling Set-Up and Assumptions

The ability of a red blood cell (RBC) to deform is a significant indicator of its viability since optimal cellular deformability is essential for both micro- and macro circulation. In order to survive in high shear stress while being forced to pass through capillaries, high deformability is a must. The deformability of RBC is primarily determined via three factors: surface area-to-volume ratio of the biconcave disc, membrane viscosity, and viscoelasticity [25, 28, 30]. In HemoCell, the RBC is represented by a discrete element model in which the material model consists of five major parameters in defining the deformability of a RBC as follows [34]:

$$Parameters = \{\kappa_V, \kappa_A, \kappa_L, \kappa_B, \eta_m, \eta\}$$

where κ_V, κ_A, κ_L, and κ_B denote volume conservation coefficient, local area conservation coefficient, link force coefficient, and a combined bending force modulus for membrane and cytoskeleton. For the ease of implementation of these coefficients in the lattice Boltzman environment, the value of these four coefficients are translated into a dimensionless value via numerical computation. The remaining two parameters η_m and η denote the membrane viscosity and dynamic viscosity, respectively.

Surface Area-to-Volume. Healthy red blood cells have a volume of approximately 90 μm3 with a surface area of approximately 136 μm^2 [9]. The shape of a healthy red blood cell as shown in Fig. 1(a) is known to be a biconcave which gives a large surface-area-to-volume ratio. This has been proven via equilibrium of forces in strong-deformation experiments which shown that the surface area-to-volume ratio of the hRBC is 40% greater than a sphere with the same volume [9]. Experimental data from detailed analysis on the cell geometry of the malaria-infected red blood cells during gametocytogenesis have revealed that the surface area-to-volume ratio for each stage was nearly constant [1]. Although significant morphology changes are observed through the maturation of gametocytes, data suggested that any changes in deformability during sexual development cannot be thought as a direct influencer in the changes of surface area-to-volume ratio for the host cell. This is because approximately 70% of the RBC hemoglobin is digested during maturation [8]. Similar results were found via cryopreserved parasites measurement in which the authors claimed that the surface area-to-volume ratio is not a key determinant in the overall deformability changes [12]. Hence, in this paper, we assume that the local area conservation of malaria-infected red blood cell with stage V gametocyte has a similar local area conservation constraint as the hRBC. Meanwhile, in HemoCell, the local area conservation is constrained via a constant dimensionless area conservation coefficient, denoted as κ_A (it is set as 5.0 during simulations).

Membrane Viscosity η_m. The RBC membrane is considered as an ultrathin two-dimensional fluid layer endowed with surface viscosity. The thickness of a hRBC is approximately 80 nm [1], while the vRBC has a thickness of approximately 70 nm

[8] which are observed via transmission electron microscope. The membrane viscosity is determined as follows where d and η denote the thickness and the fluid bilayer viscosity, respectively.

$$\eta_m = d \times \eta$$

Note that in the experimental setup using a slit-flow cytometer, the RBC has a dynamic fluid viscosity of 0.025 Pa s. Here, we assume that both the fluid bilayer viscosity and dynamic fluid viscosity are the same. Hence, the membrane viscosity for hRBC and vRBC are 5.0×10^{-10} Ns m^{-1} and 2×10^{-9} Ns m^{-1}, respectively.

Elasticity. This is one of the crucial mechanical properties of a RBC in which the lipid bilayer membranes of RBC are linked to the cytoskeleton for cellular deformability, shape recovery, flexibility, and durability. The shear modulus is one of the parameters used in determining the viscoelasticity of a cell. Data obtained via micropipette aspiration revealed that from stage II to IV, the shear moduli of each stage increase significantly, while there is a sharp drop in shear modulus during the transition of stage IV to stage V [1]. In order to implement shear modulus in HemoCell, the parameter κ_L is used. It is defined as a link force which acts along links of the numerical surface elements to model the response from stretching and shearing caused by external and internal forces [34]. Due to the complex geometry of the surface discretization, recovering the value of the Young and shear moduli corresponding to a given set of parameters is not trivial. In HemoCell, we apply an additional numerical simulation where we stretch and shear a patch of the membrane in order to obtain the module emerging from a given dimensionless κ_L value.

Force-Fitting. In a slit-flow cytometer, the vacuum-generating mechanism is connected to the slit element, where the fluid is allowed to flow through the slit and to be collected in the other end as driven by the differential pressure [23]. As the differential pressure reaches equilibrium state, the fluid stops flowing. During the changes of differential pressure, the RBC morphology changes accordingly from prolate ellipsoid to biconcave. Hence, in order to replicate the stretching forces acting on a cell inside a slit-flow cytometer, we tuned the force of cell stretching simulation and compared the results with experimental data from previous research [8].

Stage V Gametocyte Three-Dimensional (3D) Model. The *in-silico* studies allow us to further understand the mechanical properties of certain living cells in a much convenient way where we can tune the parameters and test the corresponding hypothesis observed from experiments. In this paper, the geometry of vRBC is modelled with the respective dimension measurement obtained from epifluorescence microscopy and 3D imaging as shown in Table 1.

Table 1. Dimension measurement, surface area and volume of infected red blood cells at different gametocytogenesis stages (obtained from [1])

Stage	Length	Width	Thickness	Surface area	Volume	Surface area/ volume ratio
I	6.95 ± 0.66	6.51 ± 0.79	3.34 ± 0.6	102.92 ± 10.39	71.6 ± 11.88	0.81 ± 0.08
II	8.10 ± 1.13	6.58 ± 0.54	3.02 ± 0.52	115.97 ± 14.3	76.41 ± 12.45	0.75 ± 0.05
III	9.92 ± 1.15	5.39 ± 0.86	2.99 ± 0.51	117.71 ± 17.61	78.55 ± 13.58	0.76 ± 0.03
IV	12.09 ± 1.37	4.62 ± 0.69	3.12 ± 0.58	118.71 ± 7.57	73.01 ± 6.84	0.71 ± 0.04
V	10.72 ± 1.32	4.88 ± 0.76	2.94 ± 0.38	122.92 ± 9.92	82.88 ± 10.06	0.75 ± 0.06

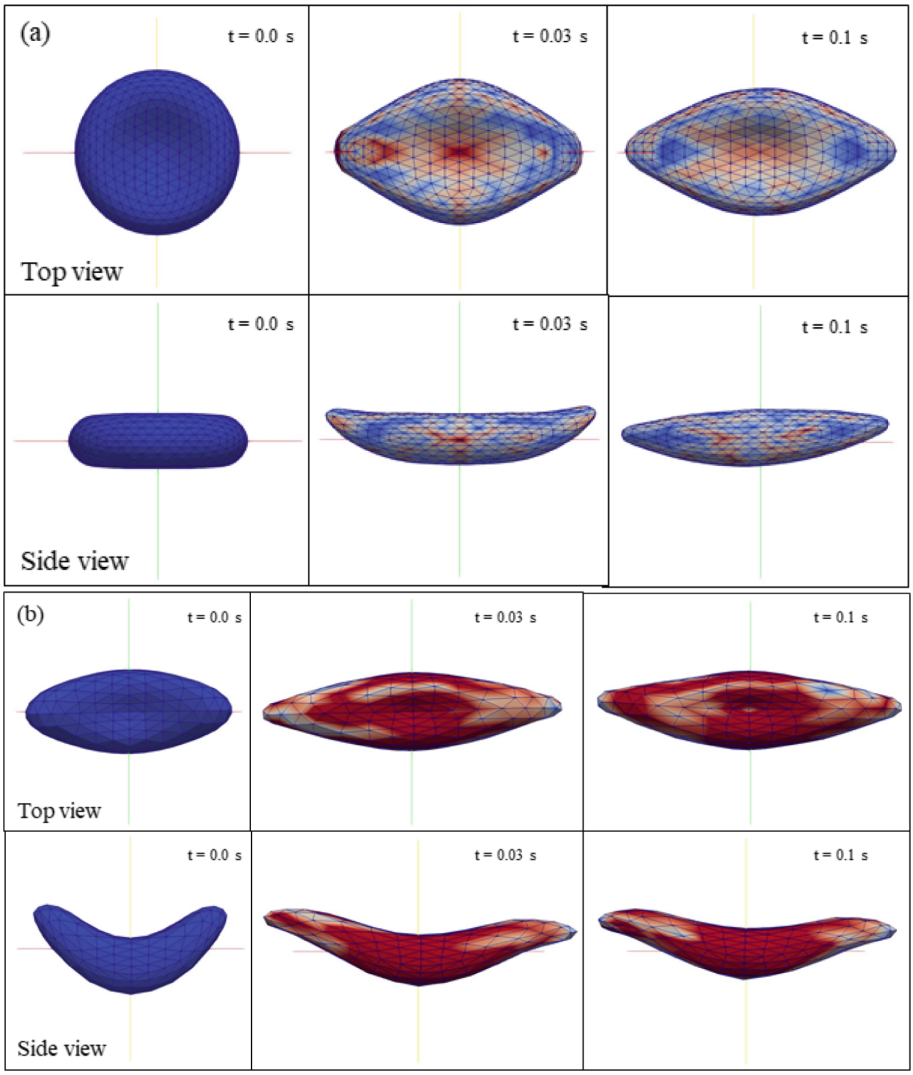

Fig. 1. Screenshots of the deformation for (a) hRBC, and (b) vRBC at different timestep.

Elongation Index. The cellular deformability for hRBC and vRBC are determined by the elongation index (EI) such that

$$EI = \frac{L - W}{L + W} \tag{1}$$

where L and W denote the length (axial) and width (transverse) diameter of the respective cell.

In the case of vRBC, as illustrated in Fig. 1(b), due to the already elongated morphology, the EI is determined as follows

$$EI = EI_t - EI_0 \tag{2}$$

Where EI_t and EI_0 denote the elongation index at time t and the initial elongation index, respectively.

3 Results and Discussion

In this study, we aim to replicate the stretching forces acting on a cell inside a slit-flow cytometer using the HemoCell framework. The parameters used in representing the cellular deformability of hRBC and vRBC are being tuned to respective optimal values that would mimic the deformability of the cell in a slit-flow cytometer. In the experiments performed by Dearnley et al. [8] where the elongation index of hRBC and vRBC are measured via slit-flow cytometer at shear stress of 3 Pa, results showed that hRBC has an elongation index of 0.34 while the vRBC has an elongation index of 0.18. In HemoCell, the parameters in defining the deformability of hRBC as shown in Table 3 has been validated in a previous study [34]. Taking the model of hRBC as a benchmark model, we tuned the respective stretching force to obtain an adequate stretching force value which gives similar elongation index for the hRBC at shear stress of 3 Pa inside a slit-flow cytometer. In the simulation, we stretched the cell with various of stretching force values for 10 ms where the elongation index is measured by using Eq. (1). As illustrated in Fig. 2, the optimal stretch force values fall in the range of 90 pN to 110 pN where the elongation index of hRBC is in the range of 0.3 to 0.35. Therefore, we selected a stretching force of 110 pN for the rest of the simulations in tuning κ_L value for the vRBC model.

As compared to Stage I to IV gametocytes, only the mature banana-shaped stage V gametocytes (vRBC) are able to move freely in the peripheral blood circulation to be uptake by the Anopheles mosquitoes [22]. Although they do not cause pathological effects on patients, they play a crucial role in disease transmission. Hence, Aingaran et al. [1] evaluated the shear modulus of different stages gametocyte using micropipette aspiration. Experiment results indicated that the shear modulus of vRBC is in the range of approximately 20 pN μm^{-1} to 120 pN μm^{-1}. The shear modulus emerging from the model using the given parameters is inferred from a numerical simulation in which a patch of the membrane is being sheared to obtain the corresponding resulting shear

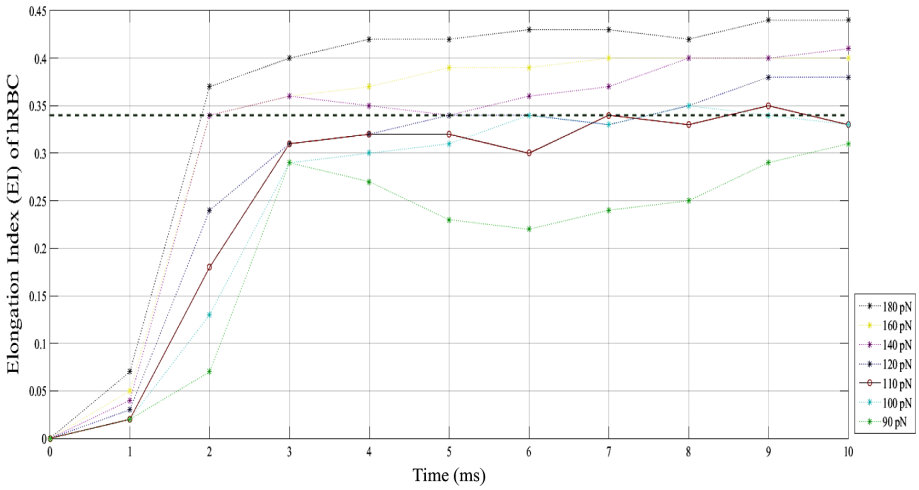

Fig. 2. Elongation index (EI) values for hRBC due to different stretching forces in the simulation, where the dotted forest-green line indicates the observed experimental data for hRBC. (Color figure online)

modulus values. Hence, secondly, in accordance to the given range of shear modulus from experimental data, we generated a set of κ_L values as shown in Table 2.

Table 2. Parameters used in the simulations.

kLink, κ_L	Shear modulus (μN m^{-1})
28	20.3
70	50.7
84	60.9
97	70.3
111	80.5
125	90.6
138	100.1
152	110.2
166	120.3

We investigated which of these κ_L values give an elongation index of 0.18 for the vRBC at a stretching force of 110 pN for 10 ms. In Fig. 3., various elongation index values are obtained via the stretching test. Note that the vRBC model with κ_L value of 28 has an elongation index of 0.18 which is in good agreement with the experimental results. Thus, the best fit κ_L parameter which define the elasticity of vRBC is 28. Figure 4 shows the final simulation results obtained from the parameters values given in Table 3.

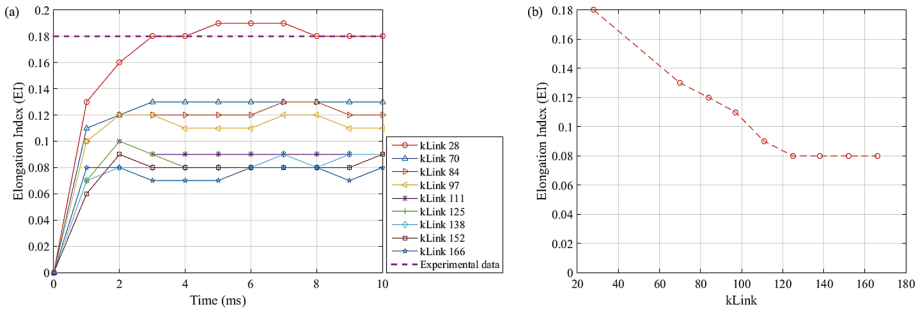

Fig. 3. The variation of the elongation index for stage V gametocyte (vRBC) at a stretching force of 110 pN for 10 ms with (a) time and (b) dimensionless κ_L values. The purple dotted-line indicates the observed experimental data for vRBC. (Color figure online)

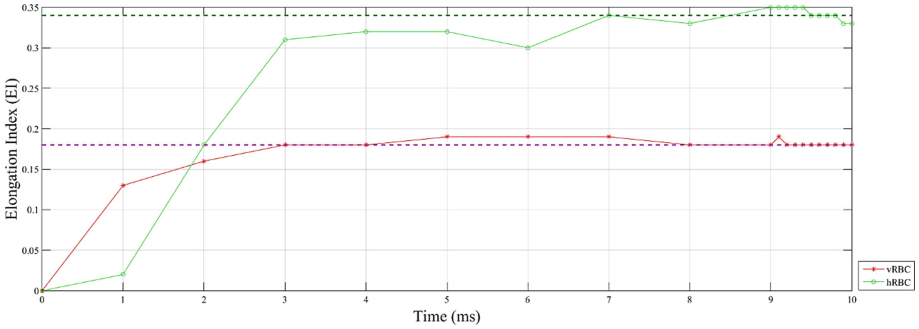

Fig. 4. The estimated elongation index values for healthy RBC and stage V gametocyte at a stretching force of 110 pN. The forest-green and purple dotted-lines indicate the observed elongation index for hRBC and vRBC, respectively. (Color figure online)

Table 3. Parameters used in simulations.

Parameters	Healthy RBC (hRBC)	Stage V gametocyte (vRBC)
kVolume	20	20
kArea	5	5
kLink	15	28
kBend	80	200
Force	110 pN	110 pN

4 Conclusion

In this study, we used Lattice Boltzmann simulations to study the stretching forces acting on a red blood cell inside a slit-flow cytometer. The parameters that represent the cellular deformability of healthy and malaria infected red blood cells are chosen such that they mimic the deformability of the cell in a slit-flow cytometer. The simulation

results show excellent agreement with the experimental data and allow for studying the transportation of malaria infected red blood cell in blood circulation. This in turn will provide a better understanding and new insights of the in-host disease development.

References

1. Aingaran, M., Zhang, R., Law, S.K., Peng, Z., Undisz, A., Meyer, E., Diez-Silva, M., Burke, T.A., Spielmann, T., Lim, C.T., Suresh, S., Dao, M., Marti, M.: Host cell deformability is linked to transmission in the human malaria parasite P. falciparum. Cell. Microbiol. **14**(7), 983–993 (2012)
2. Alowayyed, S., Závodszky, G., Azizi, V., Hoekstra, A.G.: Load balancing of parallel cell-based blood flow simulations. J. Comput. Sci. **24**, 1–7 (2018)
3. Artoli, A.M.M., Hoekstra, A.G., Sloot, P.M.A.: 3D pulsatile flow with the lattice Boltzmann BGK method. Int. J. Mod. Phys. C **13**(8), 1119–1134 (2002)
4. Artoli, A.M.M., Hoekstra, A.G., Sloot, P.M.A.: Simulation of a systolic cycle in a realistic artery with the lattice Boltzmann BGK method. Int. J. Mod. Phys. C **17**(1 en 2), 95–98 (2003)
5. Axner, L., Hoekstra, A.G., Sloot, P.M.A.: Simulating time harmonic flows with the lattice Boltzmann method. Phys. Rev. E **75**, 036709 (2007)
6. Bernaschi, M., Fatica, M., Melchionna, S., Succi, S., Kaxiras, E.: A flexible high-performance lattice Boltzmann GPU code for the simulations of fluid flows in complex geometries. Concurr. Comput.: Pract. Exp. **22**(1), 1–14 (2010)
7. Dixon, M.W., Dearnley, M.K., Hanssen, E., Gilberger, T., Tilley, L.: Shape-shifting gametocytes: how and why does P. falciparum go banana-shaped? Trends Parasitol. **28**(11), 471–478 (2012)
8. Dearnley, M.K., Yeoman, J.A., Hanssen, E., Kenny, S., Turnbull, L., Whitchurch, C.B., Tilley, L., Dixon, M.W.: Origin, composition, organization and function of the inner membrane complex of P. falciparum gametocytes. J. Cell Sci. **125**(Pt 8), 2053–2063 (2012)
9. Eggleton, C.D., Popel, A.S.: Large deformation of red blood cell ghosts in a simple shear flow. Phys. Fluids **10**(8), 1834–1845 (1998)
10. Goergen, C.J., Shadden, S.C., Marsden, A.L.: SimVascular as an instructional tool in the classroom. In: 2017 IEEE Frontiers in Education Conference (FIE), Indianapolis, IN, pp. 1–4 (2017)
11. Gross, M., Krüger, T., Varnik, F.: Rheology of dense suspensions of elastic capsules: normal stresses, yield stress, jamming and confinement effects. Soft Matter **10**, 4360–4372 (2014)
12. Hanssen, E., Knoechel, C., Dearnley, M., Dixon, M.W., Le Gros, M., Larabell, C., Tilley, L.: Soft X-ray microscopy analysis of cell volume and hemoglobin content in erythrocytes infected with asexual and sexual stages of Plasmodium falciparum. J. Struct. Biol. **177**(2), 224–232 (2011)
13. Hawking, F., Gammage, K., Worms, M.J.: Evidence for cyclic development and short-lived maturity in the gametocytes of Plasmodium falciparum. Trans. R. Soc. Trop. Med. Hyg. **65** (5), 549–559 (1971)
14. Heldt, T., Mukkamala, R., Moody, G.B., Mark, R.G.: CVSim: an open-source cardiovascular simulator for teaching and research. Open Pacing Electrophysiol. Ther. J. **3**, 45–54 (2011)
15. Hoekstra, A.G., Alowayyed, S., Lorenz, E., Melnikova, N., Mountrakis, L., van Booij, B., et al.: Towards the virtual artery: a multiscale model for vascular physiology at the physics-chemistry-biology interface. Philos. Trans. R. Soc. A **374**, 20160146 (2016)

16. Kaandorp, J.A., Lowe, C.P., Frenkel, D., Sloot, P.M.A.: The effect of nutrient diffusion and flow on coral morphology. Phys. Rev. Lett. **77**(11), 2328–2331 (1996)
17. Kandhai, D., Koponen, A., Hoekstra, A.G., Kataja, M., Timonen, J., Sloot, P.M.A.: Lattice-Boltzmann hydrodynamics on parallel systems. Comput. Phys. Commun. **111**(1–3), 14–26 (1998)
18. Krüger, T., Varnik, F., Raabe, D.: Efficient and accurate simulations of deformable particles immersed in a fluid using a combined immersed boundary lattice Boltzmann finite element method. Comput. Math. Appl. **61**, 3485–3505 (2011)
19. Krüger, T., Gross, M., Raabe, D., Varnik, F.: Crossover from tumbling to tank-threading-like motion in dense simulated suspensions of red blood cells. Soft Matter **9**, 9008–9015 (2013)
20. Krüger, T.: Effect of tube diameter and capillary number on platelet margination and near-wall dynamics. Rheol. Acta **55**, 511–526 (2016)
21. Laveran, A.: A new parasite found in the blood of malarial patients. Parasitic origin of malarial attacks. Bull. Mem. Soc. Med. Hop. Paris **17**, 158–164 (1880)
22. Lavazec, C., Alano, P.: Uncovering the hideout of malaria sexual parasites. Blood **123**(7), 954–955 (2014)
23. Moon, D., Bur, A.J., Migler, K.B.: Multi-sample micro-slit rheometry. J. Rheol. **52**(2), 1131–1142 (2008)
24. Pan, C., Prins, J.F., Miller, C.T.: A high-performance lattice Boltzmann implementation to model flow in porous media. Comput. Phys. Commun. **158**(2), 89–105 (2004)
25. Radosinska, J., Vrbjar, N.: The role of red blood cell deformability and Na, K-ATPase function in selected risk factors of cardiovascular disease in humans: focus on hypertension, diabetes mellitus and hypercholesterolemia. Physiol. Res. **65**(Suppl. 1), 43–54 (2016)
26. Salmon, R.: The lattice Boltzmann method as a basis for ocean circulation modeling. J. Mar. Res. **57**, 503–535 (1999)
27. Sinden, R.E.: Sexual development of malarial parasites. Adv. Parasitol. **22**, 153–216 (1983)
28. Tiburcio, M., Niang, M., Deplaine, G., Perrot, S., Bischoff, E., Ndour, P.A., Silvestrini, F., Khattab, A., Milon, G., David, P.H., Harderman, M., Vernick, K.D., Sauerwein, R.W., Preiser, P.R., Mercereau-Puijalon, O., Buffet, P., Alano, P., Lavazec, C.: A switch in infected erythrocyte deformability at the maturation and blood circulation of P. falciparum transmission stages. Blood **119**(24), e172–e180 (2012)
29. Thommes, G., Sea, M., Banda, M.K.: Lattice Boltzmann methods for shallow water flow applications. Int. J. Numer. Methods Fluids **55**(7), 673–692 (2007)
30. Tomaiuolo, G.: Biomechanical properties of red blood cells in health and disease towards microfluidics. Biomicrofluidics **8**(5), 051501 (2014)
31. Tran, N.-P., Lee, M., Hong, S.: Performance optimization of 3D lattice Boltzmann flow solver on a GPU. Sci. Program. **2017**, 1–16 (2017)
32. Tubbs, K.R., Tsai, F.T.C.: Multilayer shallow water flow using lattice Boltzmann method with high performance computing. Adv. Water Resour. **32**(12), 1767–1776 (2009)
33. WHO World Malaria Report (2017). http://apps.who.int/iris/bitstream/10665/259492/1/9789241565523-eng.pdf
34. Závodszky, G., van Rooij, B., Azizi, V., Hoekstra, A.: Cellular level in-silico modeling of blood rheology with an improved material model for red blood cells. Front. Physiol. **8**, 563 (2017)
35. Zhong, L., Feng, S., Lou, D., Gao, S.: Wind-driven, double-gyre, ocean circulation in a reduced-gravity, 2.5-layer, lattice Boltzmann model. Adv. Atmos. Sci. **23**(4), 561–578 (2006)

36. Zhou, J.G., Causon, D.M., Mingham, C.G., Ingram, D.M.: Numerical prediction of dam-break flows in general geometries with complex bed topography. J. Hydraul. Eng. **130** (4), 332–340 (2004)
37. Zhou, J.G.: Lattice Boltzmann simulations of discontinuous flows. Int. J. Mod. Phys. C: Comput. Phys. Phys. Comput. **18**(1), 1–14 (2007)
38. https://www.hemocell.eu